Chapter 6

Third-order Effects

We are going to focus attention on Raman laser applying the stimulated Raman scattering, one of the third-order nonlinear effects. We show the study of Nd:YVO_4 intracavity self-Raman laser and the possible solution to improve damage threshold. Following that, we demonstrate a Nd:YAG/$BaWO_4$ Raman laser with highest efficiency till then by the first use of actively Q-switching.

6.1 Thired-order Effects and Stimulated Raman Scattering

Third harmonic generation (THG), Keer effect, self-focusing, self-diffraction, self-phase modulation, spatial solitions, temporal solitions, stimulated Brillouin and thermal Brillouin scattering (SBS and STBS), stimulated Rayleigh and thermal Rayleigh scattering (SRLS and STRS), stimulated Rayleigh wing scattering (SRWS), and stimulated Raman techniques (SRS... etc.) were categorized in third-order effects. Isotropic matter of cubic symmetry does not show second-order nonlinear effects. Some particular isotropic matter such as gases, solutions and amorphous solids are able to have high-efficient third-order nonlinear effects which can be applied in photonics. [B1,B6]

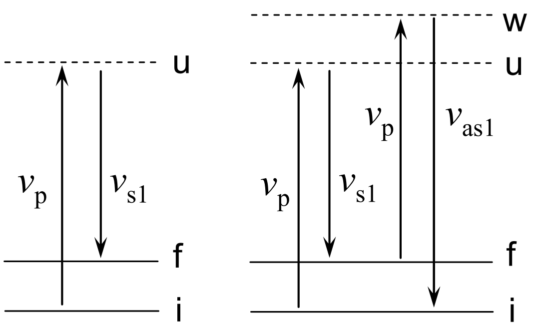

Fig. 6.1. Generation of first Stokes frequency ν_{S1} and first anti-Stokes frequency ν_{AS1} [B4].

Compared with Raman scattering which is inelastic light-scattering process, the mechanism of harmonic generation, random scattering, or optical parametric oscillation in last chapter lose almost no energy ideally. Phase-matching is considered in these nonlinear effects, but not in stimulated Raman techniques. However, this doesn't imply that the cut angle is unrelated because of the direction-dependent spectrum of Raman shift. Energy level for Raman scattering shows the first Stokes and first anti-Stokes frequency in Fig. 6.1.

6.2 Diode-pumped AQS Nd:YVO$_4$ Self-Raman Laser at 1176 nm and 1525 nm

Research on SRS is important in laser physics because of the generation of laser sources operating in new wavelengths. The rapid discovery of new Raman medium has made Raman laser a significant technology. The most efficient crystal in DPSSL, Nd:YVO$_4$, had been used as self-Raman medium in PQS and AQS all-solid-state laser since 2004 [33-34,49]. The experimental configuration showed in Fig. 6.2.

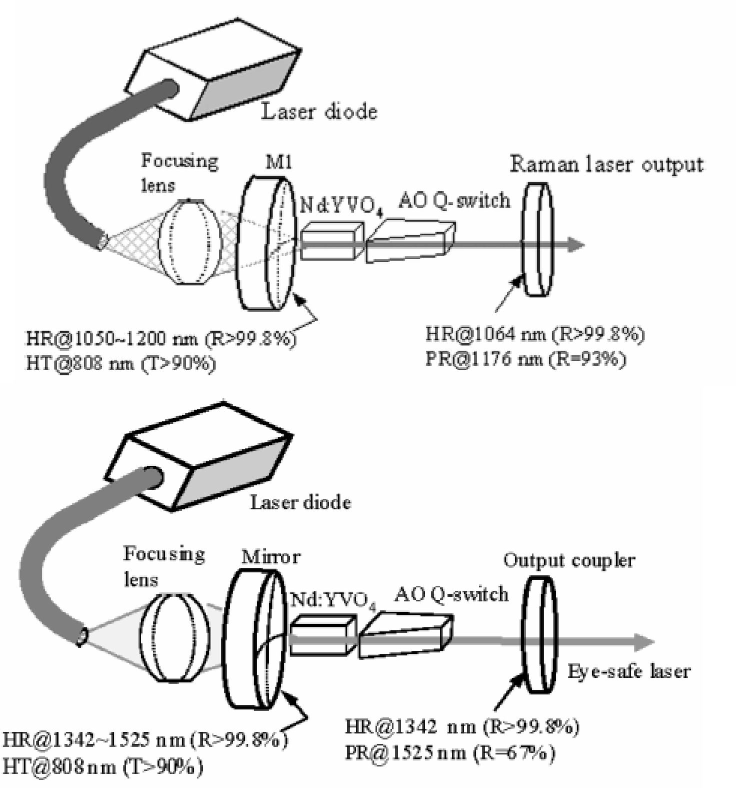

Fig. 6.2. Schematic of the diode-pumped actively Q-switched Nd:YVO$_4$ self-Raman laser.

Efficient self-Raman frequency conversion from a diode-pumped actively Q-switched Nd:YVO$_4$ laser at 1064 nm to Stokes emission at 1176 nm is achieved for the first time in [34]. With a 0.2-at.% Nd:YVO_4 crystal, greater than 1.5 W of power at a wavelength of 1176 nm at a repetition rate of 20 kHz was generated with a diode pump power of 10.8 W, corresponding to a conversion of 13.9%. Pulse width and peak power were 18 ns and 4.2 kW, respectively.

An efficient compact eye-safe laser at 1525 nm is presented by use of self-frequency Raman conversion in a diode-pumped actively Q-switched Nd:YVO_4 1342-nm laser [49]. At an incident pump power of 13.5 W, the self-stimulated Raman laser produces 1.2 W of 1525-nm average output power at a repetition rate of 20 kHz. The corresponding peak power at 1525 nm is generally greater than 10 kW for repetition rates from 5 to 20 kHz.

6.3 Power Scale-up of the Diode-pumped AQS Nd:YVO_4 Raman Laser with an undoped YVO4 crystal as a Raman shifter

Since the development of new Raman crystals in the last decade [1-11], the stimulated Raman scattering (SRS) in crystal [12] has provided solid-state lasers with an important way to be operated in different wavelengths. The most commonly known materials for SRS are $Ba(NO_3)_2$ [13], $LiIO_3$ [14], $KGd(WO_4)_2$ [15], $PbWO_4$ [16], and $BaWO_4$ [5,6,17-21]. Moreover, for self-Raman lasers, the materials such as Yb:$KGd(WO_4)_2$ [22], Nd:$KGd(WO_4)_2$ [23-29], Nd:$PbWO_4$ [30], Nd:$Gd_xY_{1-x}VO_4$ [31,32], Nd:$PbMoO_4$ and Nd:$SrMoO_4$ [11] have been reported. Combination of their laser-emission and SRS properties made these crystals charming self-Raman media. Nevertheless, the Raman scattering was generated by host material. Is there more important advantage of combing laser and Raman crystal except compact and short laser cavity? The lasers could offer a number of advantages if the SRS could be transferred from self-Raman media to additional undoped crystals.

Nd-doped YVO_4 and $GdVO_4$ crystals, the acknowledged useful gain media, were used in passively Q-switched (PQS) and actively Q-switched (AQS) self-Raman lasers [32-37]. For instance, an AQS Nd:YVO_4 self-Raman laser demonstrated the average power, pulse width and peak power of 1.5 W, 18 ns and 4.2 kW for the Stokes wavelength of 1176 nm [34]. In PQS Nd:$GdVO_4$ self-Raman lasers, the average power, pulse width and peak power were found to be 83 mW, 500 ps, and 9.2 kW at 1174 nm in [35], or 140 mW, 750 ps, and 8.4 kW at 1176 nm in [36]. However, the damage restricted the output properties [37] and occasionally happened in self-Raman medium even under moderate operation. For better performance in applications such as the 588-nm yellow laser for biomedicine or trying pushing to close 589-nm high power laser for artificial star, we need to extend the limit.

In this work, we report a new design of a diode-pumped AQS 1176-nm

$Nd:YVO_4$ Raman laser to increase the average power, repetition rate, peak power, and damage threshold comprehensively. An undoped YVO_4 crystal as a Raman shifter was put in the $Nd:YVO_4$ Raman laser. With an incident pump power of 18.7 W, the average power is greater than 2.6 W at 80 kHz. The pulse width of the pulse envelop is shorter then 5 ns with mode-locked modulation. With an incident pump power of 12.7 W, the pulse energy and peak power is higher than 43 μJ and 14 kW at 40 kHz.

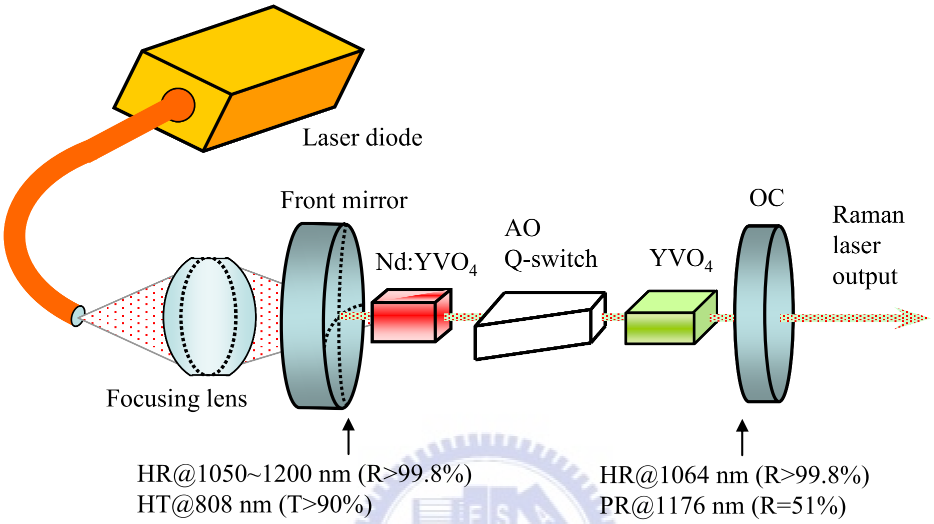

Fig. 6.3. Schematic of a diode-pumped actively Q-switched $Nd:YVO_4$ Raman laser at 1176 nm.

Figure 6.3 shows the experiment configuration for AQS $Nd:YVO_4$ 1176-nm Raman laser which differs from self-Raman laser. The pump source was an 808-nm fiber-coupled laser diode with the core diameter of 800 μm, the numerical aperture of 0.16, and the maximum output power of 25 W. A focusing lens unit with a 85% coupling efficiency was used to reimage the pump beam into the gain medium with a pump spot radius of 400 μm. The gain medium, a 9-mm-long a-cut $Nd:YVO_4$ crystal with low concentrations, 0.25 at. %, was used to reduce thermally induced fracture [34]. Both sides of this laser crystal were coated for antireflection (AR) at 1.06 μm (R<0.2%). The Raman crystal was a 9.6-mm-long a-cut undoped YVO_4 crystal. These two crystals were both wrapped with indium foil and mounted in water-cooled copper blocks individually. The 30-mm-long acousto-optic (AO) Q switch (NEOS Technologies) had AR coating at 1064 nm on both faces and was driven at a 27.12-MHz center frequency by 15 W of RF power. The resonator was a plano-concave configuration. Front mirror, a 500-mm radius-of-curvature concave mirror, was coated with AR coating at 808 nm (R<0.2%) on the entrance face, and with high-reflection (HR) coating at 1064 nm (R>99.8%) and high-transmission (HT) coating at 808 nm (T>90%) on the other face. The coating of front mirror at 1176 nm was high-reflection, too. The output coupler (OC) was a flat mirror with HR coating at 1064 nm (R>99.8%) and partial-reflection (PR) coating at 1176 nm (R=51%). The cavity length was around 115 mm and depended on pumping power. The spectrum of laser output was monitored by an optical spectrum analyzer (Advantest Q8381A, including a diffraction lattice monochromator) with a resolution of 0.1 nm. The temporal behaviors for fundamental and Raman pulses were recorded by a LeCroy digital oscilloscope (Wavepro 7100, 10 Gs/s, 1-GHz bandwidth) with two fast p-i-n photodiode and an interference filter allowing transmission only at 1064 nm.

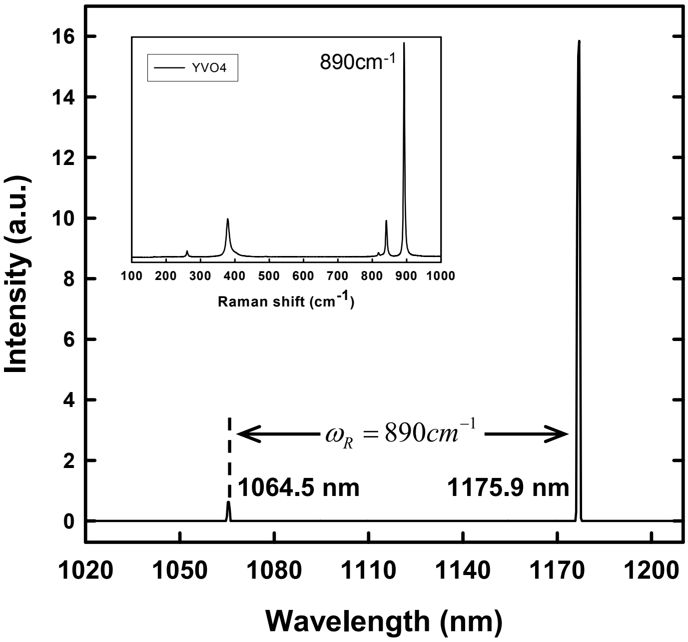

Fig. 6.4. Optical spectrum of the actively Q-switched Raman output. The Raman scattering spectrum of an YVO_4 crystal showed in inset, which is almost the same as it of $Nd:YVO_4$ crystal.

As a stimulated Raman material, taking the place of $Nd:YVO_4$ by undoped YVO_4 has advantages on robustness and output properties. Figure 6.4 displays the experimental result for optical spectrum of the laser output and Raman scattering spectrum of the YVO_4. The first Stokes wavelength near 1176 nm was conversed from the fundamental wavelength near 1064 nm by Raman peak at 890 cm^{-1}. The Raman shift of $Nd:YVO_4$ and undoped YVO_4 were almost the same, came from the same periodic YVO_4 lattice. But crystals without dopant had more perfect lattice, which brought on higher damage threshold and more stable frequency conversion. So, we can put the pure YVO_4 as a Raman crystal in the position where the intensity is highest in the cavity, and still increase the pumping power. Further, the reflectance of OC can be lower (from 93% to 51%) to scale up average output power due to lower lasing threshold at Raman wavelength. By using lower reflection coating we can narrow the pulse width, too. At the same time, when we over drove current during the experiment, the damage never happened in $Nd:YVO_4$, but in Raman crystal. That means the SRS was generated mainly in pure YVO_4, a more reliable and replaceable component in practical laser.

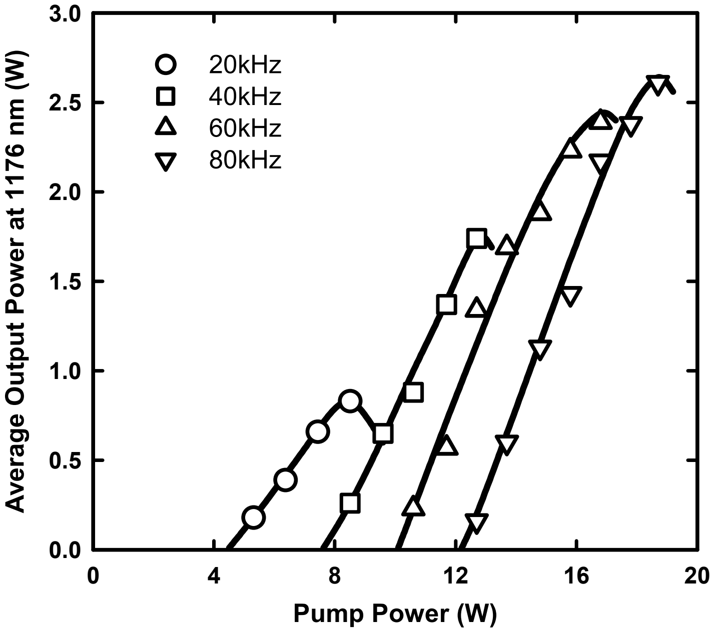

Fig. 6.5. The average output power at the Stokes wavelength of 1176 nm with respect to the incident pump power at different pulse repetition rate from 20 kHz to 80 kHz.

Figure 6.5 and figure 6.6 illustrate the output performance of AQS 1176-nm $Nd:YVO_4$ Raman laser. The average output power at the Stokes wavelength of 1176 nm with respect to the incident pump power for different pulse repetition rate of 20, 40, 60, and 80 kHz shown in Figure 6.5. Because the thermal loading of the end-pumped Q-switched Nd-doped laser increases with decreasing repetition rate [23], it can be seen that although the pumping threshold is higher, increasing the pulse repetition rate can efficiently increase the maximum average output power at 1176 nm and its maximum pump power ($P_{p,max}$). And for a certain repetition rate, to pump over $P_{p,max}$ will get the unstable Raman conversion and fall the output power. The average output power is up to 2.61 W with an incident pump power of 18.7 W at a repetition rate of 80 kHz, corresponding to the conversion efficiency of 14% and slope efficiency of 40%. Comparing to results of 1176-nm self-Raman laser by use of Nd:YVO_4 with lower dopant concentration of 0.2 at.% [34], this Raman laser still has the increase of ratio in average power of 74% and in conversion efficiency of 0.7%. It could be better if we were able to use 0.2 at.% Nd:YVO_4 and correctly AR-coated c-cut [39] YVO_4 in this Raman laser. On the other hand, the maximum pulse energy is generally greater then 40 μJ at repetition rate from 20 to 60 kHz, and up to 43.5 μJ at 40 kHz with an incident pump power of 12.7 W. The maximum pulse energy at repetition rate of 80 kHz is 32.6 μJ.

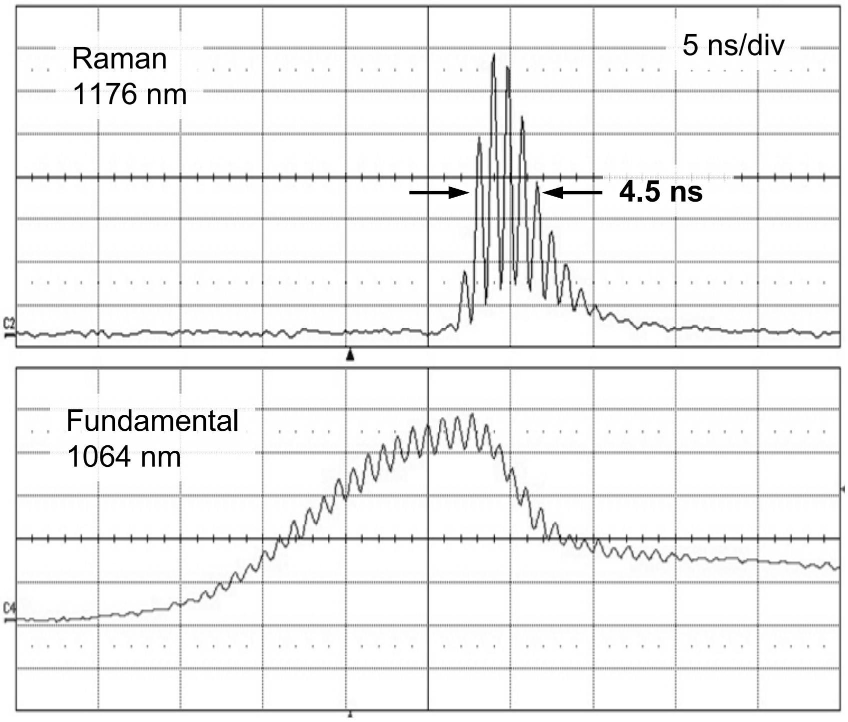

Fig. 6.6. An oscilloscope trace with mode-locking effect for fundamental and Raman pulses.

The typical time traces for fundamental and Raman pulses are shown in Figure 6.6. The pulse width is always shorter then 5 ns, but the effective pulse width is much shorter due to mode-locked shape. With the pulse energy of 43.5 μJ, the pulse width of the pulse envelop in Figure 6.6 is 4.5 ns, and the peak power of the pulse seen as a Gaussian shape should be 9.7 kW. However, after curve fitting for the mode-locked shape, the peak power is enhanced to 14 kW, 1.45 times the 9.7 kW. In other words, the effective pulse width is around 3.1 ns which is much shorter than 18 ns of self-Raman laser. Comparing to 1176-nm Nd:YVO_4 self-Raman laser of 4.2 kW, this Raman laser has more than 3 times the peak power.

In conclusion, via replacing the role of gain medium as a self-stimulated Raman crystal by undoped YVO_4 as a stimulated Raman crystal, we substantially improve the performance of AQS Nd:YVO_4 Raman lasers at 1176 nm.

6.4 Efficient Diode-pumped AQS Nd:YAG/$BaWO_4$ Intracavity Raman Laser

The development of new Raman crystals has generated a resurgence of interest in solid-state Raman lasers [3,10]. Up to now, the important Raman crystals for the realization of stimulated Raman scattering (SRS) comprise nitrates ($Ba(NO_3)_2$) [40,13], calcites ($CaCO_3$) [40,13], iodates ($LiIO_3$) [14,41], molybdates ($SrMoO_4$, $CaMoO_4$) [42], vanadates (YVO_4, $GdVO_4$) [31,34,37], and tungstates ($KGd(WO_4)_2$, $BaWO_4$, $CaWO_4$, $PbWO_4$) [43-46]. Among the tungstate crystals, $BaWO_4$ is regarded as a promising Raman-active crystal suitable for a wide range of pumping pulse duration from picoseconds to nanoseconds [47].

Although the most widespread approach for SRS is based on the external cavity configuration, intracavity SRS systems take advantage of the high intensity inside the laser cavity and use the multiple round trips of the pump laser inside the Raman cavity to increase the effective interaction length. Recently, Černý et al reported a compact quasi-CW diode-pumped passively Q-switched Nd:YAG/$BaWO_4$ Raman laser with an overall conversion efficiency of 4.4% from diode laser input power to Raman output power [47,48]. However, the performance of actively Q-switched intracavity Raman lasers based on $BaWO_4$ crystal is not yet realized.

In this section we present the first results on the efficient intracavity $BaWO_4$ SRS generation in a compact actively Q-switched diode-pumped Nd:YAG laser. At an incident pump power of 9.2 W, the compact intracavity SRS system, operating at 20 kHz, produces average output powers at 1181 nm up to 1.56 W and peak power greater than 3 kW.

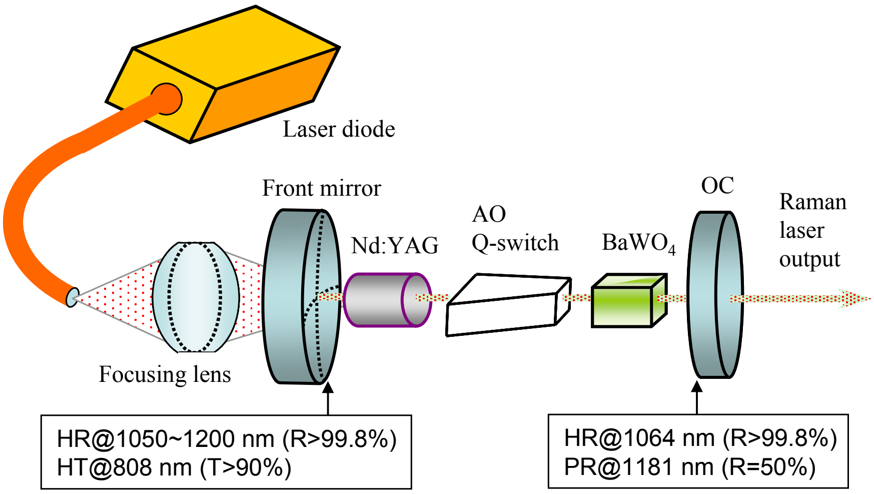

Fig. 6.9. Schematic of a diode-pumped actively Q-switched Nd:YAG/BaWO$_4$ intracavity Raman laser.

Figure 6.9 depicts the experimental configuration for the diode-pumped actively Q-switched Nd:YAG/BaWO$_4$ Raman. The cavity mirrors have special a dichroic coating for efficient conversion at the first Stokes component in an intracavity Raman configuration. The input mirror is a 500-mm radius-of-curvature concave mirror with antireflection coating at 808 nm on the entrance face (R<0.2%), high-reflection coating at 1000-1200 nm (R>99.8%) and high-transmission coating at 808 nm on the other surface (T>90%). The output coupler is a flat mirror with high-reflection coating at 1064 nm (R>99.8%) and partial-reflection coating at 1181 nm (R=50%). Note that the output coupler reflectivity is not optimized and it is limited in availability.

The pump source was an 808-nm fiber-coupled laser diode with a core diameter of 800 μm, a numerical aperture of 0.16 and a maximum output power of 10 W. A focusing lens system with 12.5-mm focal length and 90% coupling efficiency was used to re-image the pump beam into the laser crystal. The waist radius of the pump beam was approximately 300 μm. The laser medium was a 0.8-at.% Nd^{3+}:YAG crystal with a length of 10 mm. The Raman active medium was an *a*-cut BaWO$_4$ crystal with a length of 10 mm. Both sides of the Nd:YAG and BaWO$_4$ crystals were coated for antireflection at 1000-1200 nm (R<0.2%). Furthermore, both crystals were wrapped with indium foils and mounted in water-cooled copper blocks, respectively. The water temperature was maintained at 25°C. The 30-mm-long acousto-optic Q-switch (NEOS Technologies) had antireflection coatings at 1064-nm on both faces and was driven at a 27.12 MHz center frequency with 15.0-W of rf power. The overall laser cavity length was approximately 10 cm.

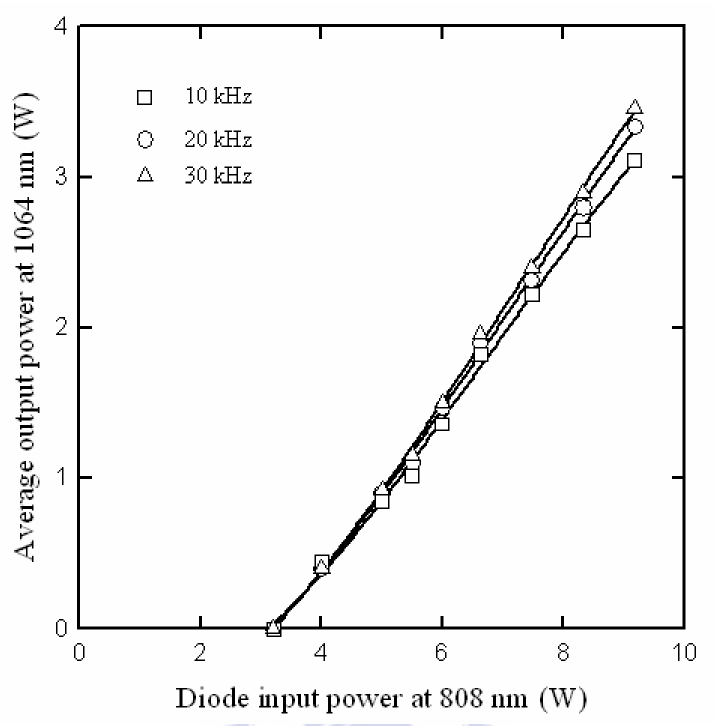

Fig. 6.10. Average output power at 1064 nm with respect to the incident pump power for pulse repetition rates of 10, 20, and 30 kHz.

The diode-pumped Q-switched Nd:YAG laser performance at 1064 nm was firstly studied for evaluating the optical-to-optical conversion efficiency of the intracavity SRS. For this investigation, an output coupler with partial reflection at 1064 nm was used instead of the above-mentioned Raman cavity output coupler. The optimum reflectivity of the output coupler was found to be approximately 80%. Figure 6.10 depicts the average output power at 1064 nm with respect to the incident pump power at the pulse repetition frequencies (PRF) of 10, 20, and 30 kHz. The threshold for 1064-nm oscillation was approximately 3.2 W and insensitive to the PRF. With an incident pump power of 9.2 W, the average output powers at 1064 nm were 3.3-3.5 W for PRFs in the range of 10-30 kHz.

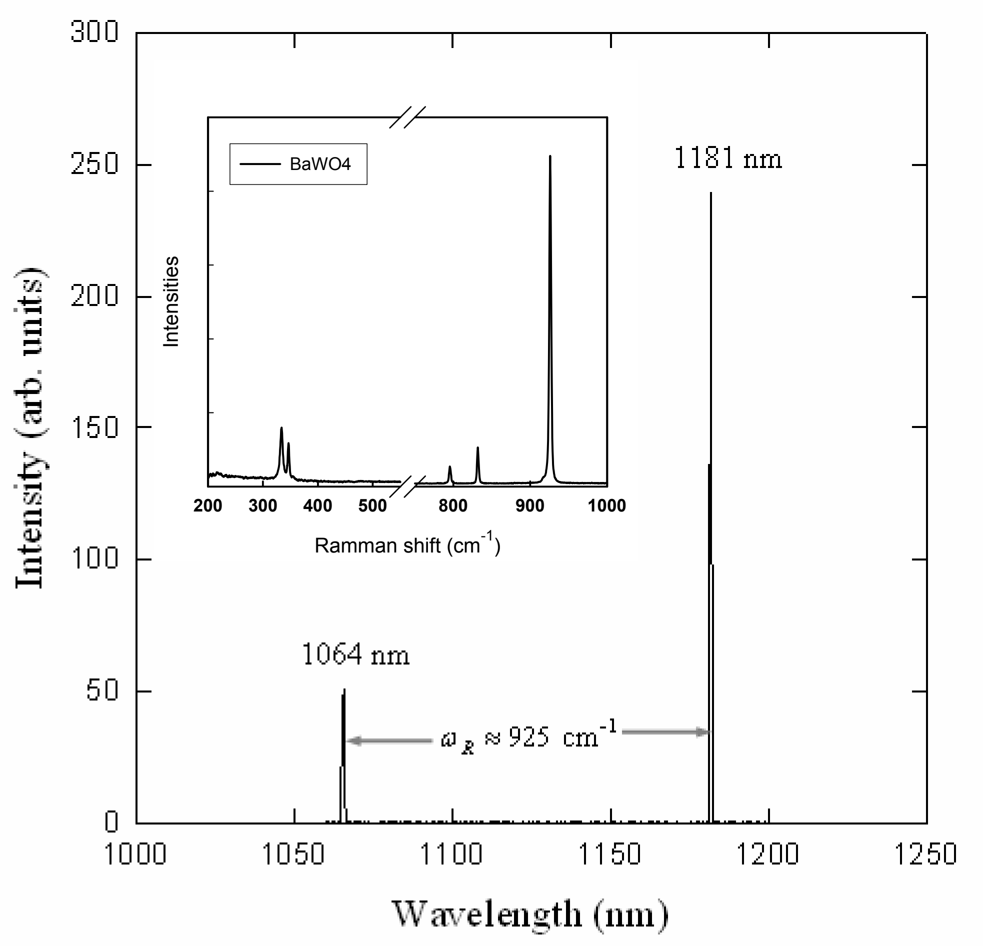

Fig. 6.11. Optical spectrum for the actively Q-switched intracavity Raman laser.

When the intracavity Raman laser was performed, the pumping threshold for the Raman laser output was found to be strongly dependent on the PRF. The spectral information of the intracavity SRS output was measured by an optical spectrum analyzer (Advantest Q8381A) that employs a diffraction grating monochromator to measure high-speed light pulses with the resolution of 0.1 nm. Figure 6.11 depicts the optical spectrum for the actively Q-switched Nd:YAG/$BaWO_4$ SRS output. It can be seen that the frequency shift between Stokes and laser lines agrees very well with the optical vibration modes of tetrahedral WO_4^{2-} ionic groups (925 cm^{-1}). Figure 6.12 shows the average output power for the intracavity SRS laser at 1181 nm as a function of the incident pump power for PRFs of 10, 20, and 30 kHz. The output polarization was found to be along the *c* axis of the BaWO4 crystal. For all pump powers, we did not observe the 2nd Stokes. The output power at the fundamental wavelength was found to be on the order of tens of mW. Even though reducing the PRF leads to a lower threshold for Raman output, experimental results revealed that self-focusing-induced damage to the volume of the $BaWO_4$ Raman crystal usually occurred at a lower PRF. Self-focusing damage in the $BaWO_4$ Raman crystal was often induced by finely adjusting the cavity alignment or slightly changing the pump beam for the optimum output. For example, the critical pump power related to the damage threshold induced by self-focusing was found to be approximately 8 W at a PRF of 10 kHz. Nevertheless, the average output power at 1181 nm was found to be up to 1.56 W at a PRF of 20 kHz with an incident pump power of 9.2 W, corresponding to a conversion efficiency of 47% with respect to the output power available from the fundamental laser of 1064 nm under optimum conditions. As a consequence, the conversion efficient from diode laser input power to Raman output power was 16.9% at a PRF of 20 kHz. To our knowledge, this is the highest efficiency for a $BaWO_4$ Raman laser reported to date.

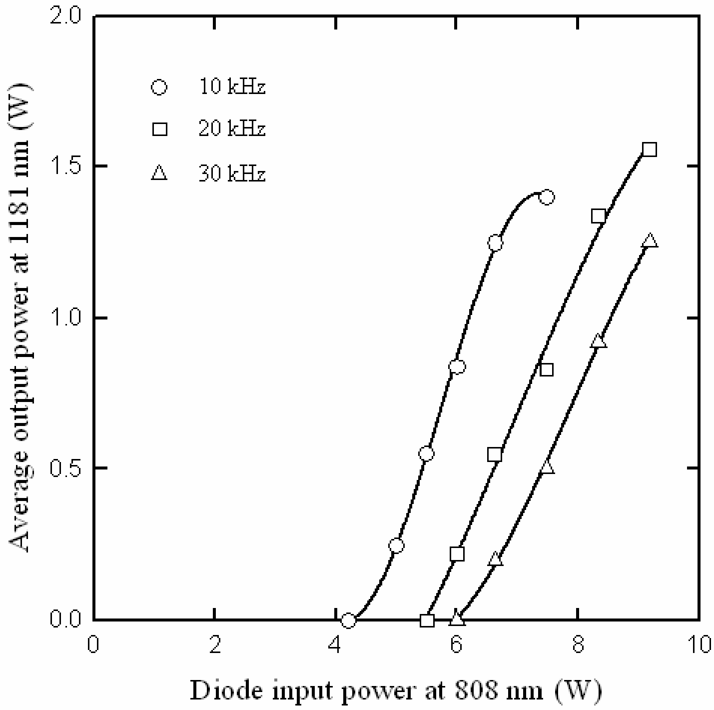

Fig. 6.12. Average output power at the Stokes wavelength of 1181 nm with respect to the incident pump power for pulse repetition rates of 10, 20, and 30 kHz.

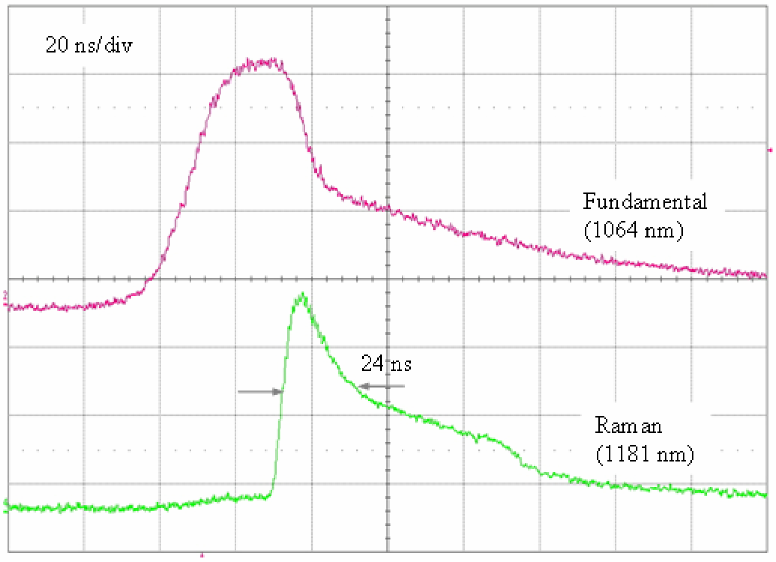

Fig. 6.13. Typical oscilloscope traces for the fundamental and Raman pulses.

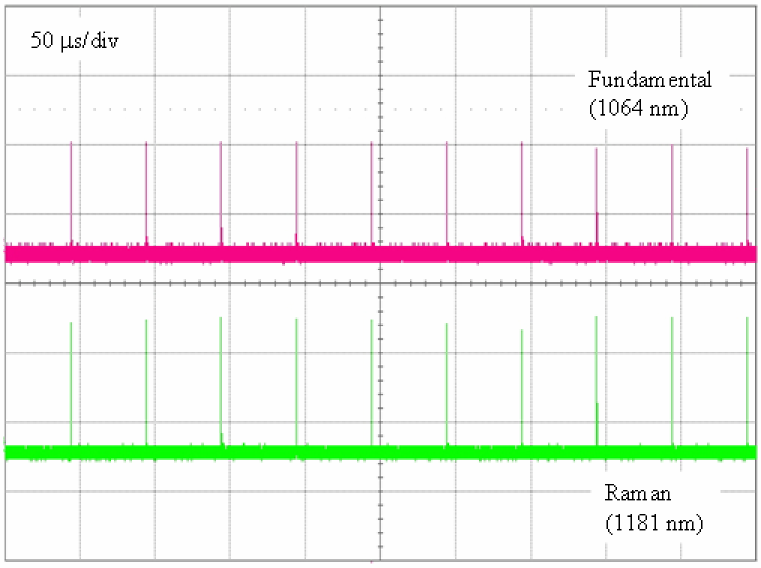

Fig. 6.14. Oscilloscope traces of a train of the fundamental and Raman output pulses.

The pulse temporal behavior was recorded by a LeCroy digital oscilloscope (Wavepro 7100, 10 Gsamples/s, 1 GHz bandwidth) with a fast p-i-n photodiode. The typical time shapes for the fundamental and Raman pulses are shown in Fig. 6.13.

The pulse duration of the Raman output was approximately 24 ns. As a consequence, the peak power was found to be higher than 3.2 kW. Oscilloscope traces of a train of the output pulses are shown in Fig. 6.14. The pulse-to-pulse amplitude fluctuation was found to be within ±10%.

In summary, A barium tungstate ($BaWO_4$) is employed to achieve efficient stimulated Raman scattering conversion in a compact diode-pumped actively Q-switched Nd:YAG laser. With an incident pump power of 9.2 W, 1.56 W of 1181-nm first Stokes average output power was generated at a pulse repetition rate of 20 kHz, corresponding to an optical-to-optical conversion efficiency of 16.9%.

6.5 Conclusion and Future Work

Via replacing the role of gain medium as a self-stimulated Raman crystal by undoped YVO_4 as a stimulated Raman crystal, we substantially improve the damage threshold, repetition rate, average output power, pulse width, and the peak power of AQS Nd:YVO_4 Raman lasers at 1176 nm. With an incident pump power of 18.7 W, the average power is 2.61 W at 80 kHz correspond to the optical-to-optical conversion efficiency of 14%. Coming with the mode-locked pulse shape, the effective cavity dump of intracavity SRS leads to peak power at 1176 nm that is generally greater than 10.5 kW at repetition rate from 20 to 80 kHz. With an incident pump power of 12.7 W, the pulse energy and peak power is higher than 43.5 μJ and 14 kW at 40 kHz.

The successful power scale-up could also be used for eye-safe Nd:YVO_4 Raman laser. Nd:YVO_4 and Nd:YAG Raman laser with an undoped YVO4 crystal as a Raman shifter is under way. Besides that, we found weak frequency tripling (third harmonic generation) in undoped YVO_4 crystal simultaneously.

And, an efficient high power diode-pumped actively Q-switched Nd:YAG/$BaWO_4$ intracavity Raman laser has been demonstrated. With an incident pump power of 9.2 W, as much as 1.56 W of average power at the Stokes wavelength was generated at a pulse repetition rate of 20 kHz, corresponding to an optical-to-optical conversion efficiency of 16.9%. Experimental results indicate that the effect of self-focusing-induced damage is a critical issue for the power scale-up of intracavity SRS. Nevertheless, the practicability of producing long $BaWO_4$ crystal provides the possibility of CW Raman laser.